The kinetics of elementary thermal reactions in heterogeneous catalysis

G. Barratt Park[1,2], Theofanis Kitsopoulos[2,5,6], Dmitriy Borodin[1], Kai Golibrzuch[2], Jannis Neugebohren[1], Daniel J. Auerbach[2], Charles T. Campbell[4] & Alec M. Wodtke[1,2,3]*

[1]Institute for Physical Chemistry, Georg-August University of Goettingen, Tammannstraße 6, 37077 Göttingen, Germany.

[2]Department of Dynamics at Surfaces, Max Planck Institute for Biophysical Chemistry, Am Faßberg 11, 37077 Göttingen, Germany.

[3]International Center for Advanced Studies of Energy Conversion, Georg-August University of Goettingen, Tammannstraße 6, 37077 Göttingen, Germany.

[4] Department of Chemistry, University of Washington, Seattle, WA 98195-1700, USA

[5] Department of Chemistry, University of Crete, Heraklion, Greece

[6] Institute of Electronic Structure and Laser – FORTH, Heraklion, Greece

*email: alec.wodtke@mpibpc.mpg.de

KEYWORDS: Ion-imaging, velocity-resolved kinetics, CO oxidation, heterogeneous catalysis, slice ion-imaging, molecular beams, surface chemistry.

Abstract

The kinetics of elementary reactions is fundamental to our understanding of catalysis. Just as micro-kinetic models of atmospheric chemistry provided the predictive power that led to the Montreal protocol reversing loss of stratospheric ozone, pursuing a micro-kinetic approach to heterogeneous catalysis has tremendous potential for societal impact. However, developing this approach for catalysis faces great challenges. Methods for measuring rate constants are quite limited and present predictive theoretical methods remain largely un-validated. This paper presents a short perspective on recent experimental advances in our ability to measure the rates of elementary reactions at surfaces that rely on a stroboscopic pump-probe concept for neutral matter. We present the principles behind successful measurement methods and discuss a recent implementation of those principles—velocity resolved kinetics. The topic is discussed within the context of a specific but highly typical surface reaction: CO oxidation on Pt, which despite more than forty years of study, was only clarified after experiments with velocity-resolved kinetics became possible. This *deceptively simple* reaction illustrates fundamental lessons concerning the coverage dependence of activation energies, the nature of reaction mechanisms involving multiple reaction sites, the validity of transition state theory to describe reaction rates at surfaces, and the dramatic changes in reaction mechanism that are possible when studying reactions at low temperatures.

Introduction

The importance of heterogeneous catalysis is exemplified by the problems of treating automobile exhaust. Our transport needs are largely fulfilled through fossil fuel combustion. Among combustion's many problems, its exhaust is poisonous. Catalytic surface chemistry is used to remove these poisons by converting them to less harmful chemicals (*e.g.* CO to CO_2 and NO_x to N_2 and H_2O). How well these catalysts work is literally a matter of life and death; it has been reported that tens of thousands of premature deaths per year could be avoided if on-road performance of catalysis matched laboratory test performance[1].

Heterogeneous catalysis also has enormous financial impacts on business suggesting that research in heterogeneous catalysis has calculable monetary value; problems arising in commercial catalysis that could, in principle, be solved through research can result in costs on the order of 100s of billions $US. In May 2014, scientists discovered evidence of 'defeat-devices' on Volkswagen automobiles, running the most modern technology for catalytic NO_x removal[2]. These discoveries eventually led to VW being prosecuted under US law. Fortune magazine reported in 2018 that costs associated with settlement of these prosecutions have reached 35 Billion $US[3]. In the meantime, lawsuits from major shareholders continue and class action lawsuits in Europe loom. Worldwide costs to VW in 2016 and 2017 were estimated to be more than 130 billion $US[4]. Prospective costs are difficult to estimate, but loss of US market share and damage to its brand both remain likely long-term outcomes.

Although existing technologies are capable of almost complete NO_x conversion, they require a fuel penalty (in the case of Lean NO_x Traps) or the consumption of a reductant (in the case of Selective Catalytic Reduction Systems). Why company leaders made decisions to circumvent emissions regulations will become a question discussed in business schools and ethics classes for years to come; however, one thing is clear: had more efficient, easy-to-implement catalytic technology been available to address the NO_x emission of diesel engines, discussion of these dubious decisions would never have reached the board rooms of major automobile companies. Why then were there no such easy-to-implement technologies available?

Despite more than a century of research into heterogeneous catalysis, the search for improved catalysts remains an empirical effort characterized by the expression "cook and look". Although fundamental insights have been obtained and there are reasons to be optimistic that predictions of new catalysts[5] will become more common, for now, most commercial catalyst developments can only be indirectly connected to basic understanding derived from fundamental research.

There is no reason that this must persist. Examples exist of complex problems in catalytic chemistry that have been understood at a fundamental level leading to great societal benefit. Consider another chemical reactor; as in automobile exhaust chemistry, catalysis also plays a defining role in the Earth's atmospheric chemistry[6]. The critical breakthrough in atmospheric chemistry came from advances in chemo-kinetic models. Knowledge of the rates of a large number of the most important reactions in the atmosphere led to a clear understanding of the role played by trace atmospheric contaminants in the balance of the Earth's atmosphere. For example, we now know that anthropogenic chlorofluorocarbons—although present in only tiny abundance—destroy the Earth's stratospheric ozone layer. We also understand why NO_x emission from automobiles under the right conditions results in excess ozone in the troposphere, posing a health threat in areas of high traffic congestion.

The development of today's chemo-kinetic models of the atmosphere required decades of work by many researchers. While the price was high, the understanding that was derived was extremely valuable, leading to passage of the *Montreal Protocol on Substances that Deplete the Ozone Layer*, regulating use of freons on a global scale. And these changes are yielding fruits—recent studies show the onset of stratospheric ozone recovery[7].

This example shows that the chemistry research community is capable of developing a predictive understanding of complex catalytic systems. Why have we not so far also developed chemo-kinetic models for heterogeneous catalysis? Researchers in this field will point to many challenges, but one of the most daunting is our current limitations in accurately measuring or theoretically predicting the rates of *elementary* thermal reactions in heterogeneous catalysis. Simply put, the kinetics of heterogeneous catalysis is hard.

What are the reasons for this?

Consider the example of NO_x removal from automobile exhaust; catalytic surface chemistry on platinum, vanadium oxide and other materials is used[8]. In this case, we have not yet identified all of the elementary chemical reactions involved, nor have we measured the rates of the ones that have been identified. Moreover, multiple reaction sites are typically found on catalytic surfaces and many of these reaction sites remain unidentified. Beyond experiment, theoretical approaches to modeling reaction rates could be used, but when rate measurements are so challenging, how can we know that theories yield reliable results?

In contrast, in the case of atmospheric chemistry, rates of elementary reactions can be obtained by a variety of well proven methods. For example, photodissociation of a free radical precursor

molecule with a short laser pulse (flash photolysis) can be used to initiate the reaction and the radical's lifetime in the presence of a known concentration of a chosen reactant can be measured by time resolved absorption spectroscopy. These "pump-probe" methods have been widely used to measure gas-phase reaction rates—for a representative review, see Ref. 9. When reaction rates cannot be measured directly, theoretical predictions can often be made using another powerful option: electronic structure calculations and transition state theory[10]. Furthermore, since these systems have few atoms and many experimental rates are available for validation, the reliability of theoretical predictions is high and well understood.

Analogous methods for measuring or predicting the rates of elementary thermal reactions at surfaces are either lacking or unproven. Flash photolysis cannot be used to initiate most surface reactions since reactant adsorption to the solid catalyst is the much more typical initiation step; it is the first step of the Langmuir-Hinshelwood mechanism. Methods for following the time evolution of reaction intermediates on two-dimensional surfaces also require higher intrinsic sensitivity than for three-dimensional gases. Finally, the theoretical foundations necessary to predict the rates of surface reactions are not yet fully established since so many atoms are involved[11-13]. Surface chemistry also provides an additional complication not present in gas phase reactions—while a gas phase collision is fundamentally homogenous, heterogeneous catalysis even on the simplest catalysts often occurs at multiple reaction sites and reactants may not fully mix.

This helps explain why greater progress had not already been made at the time of the now infamous decisions to program defeat devices in VW automobiles.

The aim of this perspective is to show that despite the daunting challenges, recent advances, both on the experimental and theoretical sides, foster optimism that we can improve our understanding and develop predictive capability needed to impact catalyst technologies.

The perspective is structured around an example reaction: CO oxidation on catalytically active single crystal Pt. This reaction has been studied for over 40 years, yet only recently has it been clearly understood. It is interesting in its own right, as it is a piece of many important technologies. It is also *deceptively simple*, providing a remarkable example of the challenges faced in measuring the rates of elementary chemical reactions on surfaces. Knowing what we now know, it is possible to see clearly the kinds of experimental principles that form the basis of successful surface kinetics and what can go wrong when these principles are not fulfilled.

We first present a discussion of these principles within the context of the CO oxidation reaction. We then show an implementation of these principles, one which led to a complete clarification of a system that presented many conflicting or ambiguous results. We use that knowledge to highlight where some classic papers in the field went wrong and why. We also point out that some of the conclusions of those classic papers must now be reconsidered. Finally, we discuss the importance of theoretical predictions of rates of elementary surface reactions. With the advent of unambiguous rate data, the moment has come for development and testing of theories and for those that pass muster, their wide-scale application.

Velocity-resolved surface kinetics

On the most basic level, kinetics of surface reactions requires us to measure the "kinetic trace": product flux, Φ, versus reaction time, τ_{rxn}. For the CO oxidation reaction, we define the kinetic trace as Φ_{CO_2} vs. τ_{rxn}. Hence, one of the most fundamental requirements of a kinetics measurement in CO oxidation surface chemistry is to measure product flux.

CO oxidation on Pt is a typical Langmuir-Hinshelwood (LH) reaction. It proceeds by adsorption and dissociation of O_2 and non-dissociative adsorption of CO followed by diffusion of CO to an O atom after which CO_2 forms and desorbs. The rate of CO_2 product formation at the surface is, by definition, a flux: the number of CO_2 molecules produced per second per cm^2. Yet, experiments normally provide signals proportional to the density of the product CO_2 molecules, $\rho_{CO_2} = \Phi_{CO_2}/v_{CO_2}$. See for example Fig. 1 from Ref. 14, where electron bombardment ionization was used to detect CO_2 product released from the surface. There, the CO_2 detection probability is proportional to the time spent by the CO_2 molecule in the ionizing electron beam, which is inversely proportional to its velocity, v_{CO_2}. In Fig. 1b, the CO_2 desorbing in the normal direction from a surface at 880 K exhibits a kinetic energy of E/k_B = 3560 K, or most probable velocity near 1.16×10^5 cm/sec. We now know that hyperthermal CO_2 is produced by the reaction occurring at 111 terraces and is a minor channel under the conditions of many previous experiments[15]. CO_2 can also be produced by other reactions occurring at steps[15]—these reactions produce velocity and

Figure 1: Hyperthermal CO_2 from CO oxidation on Pt(111). *Time of flight spectra of a) a CO molecular beam used to initiate the reaction, CO_2 reaction product detected in the direction b) normal and c) 45° to the surface normal. Such hyperthermal CO_2 has been observed at least 40 years ago; only now do we know that this is the reaction taking place at the 111 terraces. Oxygen Pressure = 1×10^{-7} Torr. T_s = 880 K. Figure adapted with permission from Ref. 14, American Institute of Physics.*

angular distributions reflecting CO_2 products that have been thermalized with the surface[16] with most probable velocities near 8×10^4 cm/sec at a surface temperature of 880 K.

The branching between the reactions resulting in thermal and hyperthermal products depends on surface O-coverage and temperature. Consider the problems arising when measuring the branching ratio between these two reactions with a number density detector and no knowledge of the velocities. If both reactions produce the same number of product molecules per second, a density detector would yield an apparent ratio of ~ 1:1.45 in favor of the thermal channel, since faster molecules appear with lower density. With measured velocities to complement a number density detector, like data shown in Fig. 1, we can correct the observed densities to obtain relative fluxes of the two channels and obtain the correct branching.

Combining a density detector with velocity measurement capability also allows the development of a pump-probe experiment applicable to LH (or indeed other surface) reactions. Pump-probe experiments are normally done with two laser light pulses. The time-resolved signal must depend on both pulses and is then measured as a function of the delay between them. Formally, the time dependent signal depends on both the flight times of the photons to the interaction zone and from the interaction zone to the light detectors. The experiment is dramatically simplified by the fact that light travels so fast and with a constant velocity; these flight times are usually negligibly small and constant. This is not so for molecules. Consider CO oxidation—here, three times must be distinguished to obtain meaningful kinetic data. First, the reaction is initiated by a pulse of CO molecules. This CO pulse must fly from the position where it is produced to the reactive surface (τ_{CO}, reactant flight-time). The reaction then takes place on the surface over a certain time, (τ_{rxn}, reaction time). Finally, desorbing products fly from the surface to the detector ($\tau_{\mathrm{CO_2}}$, product flight time). We can only observe the signal as a function of the total time, $\tau_{CO} + \tau_{rxn} + \tau_{\mathrm{CO_2}}$. Of course, only τ_{rxn} is relevant for the kinetics.

Figure 2: CO_2 product angular distribution from the CO oxidation on Pt(111). *Flux measurements were performed lacking velocity resolution. The incident molecular beam had a 1 mm diameter and the quadrupole detector had a 1 mm slit located 4 cm from the surface, resulting in an angular resolution of 2.9°. T_s = 467 K. The angular distribution depends on O-coverage, θ_o. The fits to the data are based on two contributions that exhibit a narrow and broad angular distribution. Figure drawn using data from Ref. 17.*

A final demand for accurate kinetics measurements is the ability to integrate the product flux over all angles of desorption, an aspect of the experimental challenge that CO oxidation also reveals. It is long known that the hyperthermal channel

appears with a narrow angular distribution while the thermal channel appears with a broad one. Figure 2 shows measurements of the product angular distribution, which changes with O-coverage at a constant surface temperature[17]. We now know that the narrowing of the angular distribution at higher O coverage results from increased reaction at terraces relative to steps with increasing O-coverage. While the evidence of Figure 2 may not be fully persuasive of this assertion, such conclusions become obvious with velocity resolved detection.

Implementing the principles

As far back as 1977, the time-of-flight detector used in Ref. 14 (Fig. 1) could have been used to combine product velocity information with density measurements. To our knowledge no such experiments were ever attempted. The practical difficulties that must be overcome are considerable[18]. Nowadays, it is far simpler to carry this out using ion imaging[19,20]. Figure 3 shows an instrument constructed in the Göttingen laboratory that combines ultrahigh vacuum surface science methods, molecular beams, and ion imaging.

This machine uses two pulsed molecular beams—one for CO and one for O_2—that fly in the horizontal plane to deliver reactants to the catalytic surface shown at the intersection of the two beams (left panel top view). In the right panel (side view) the implementation of ion imaging

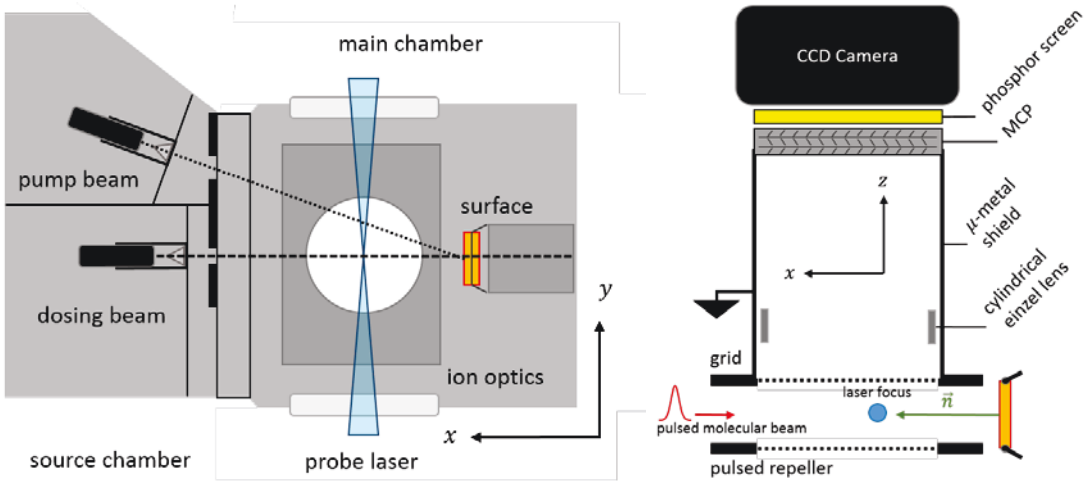

Figure 3: An instrument for velocity resolved surface reaction kinetics. *(left panel) top view of the instrument. Two molecular beams deliver reactants to the catalytic surface. Differential pumping chambers reduce the pressure to ultra-high vacuum in the main chamber. Sample preparation is performed with an Argon Ion Gun, a residual gas analyzer (RGA) and an Auger electron spectrometer. (right panel) side view of the instrument. Ion imaging detection of products provides velocity information. Non-resonant multiphoton laser ionization of products is performed with a 3 mJ, 120 fs pulse of 800 nm light and mass-specific ion detection via time-of-flight measurement is enabled by pulsing the voltage on the multichannel plate (MCP) detector.*

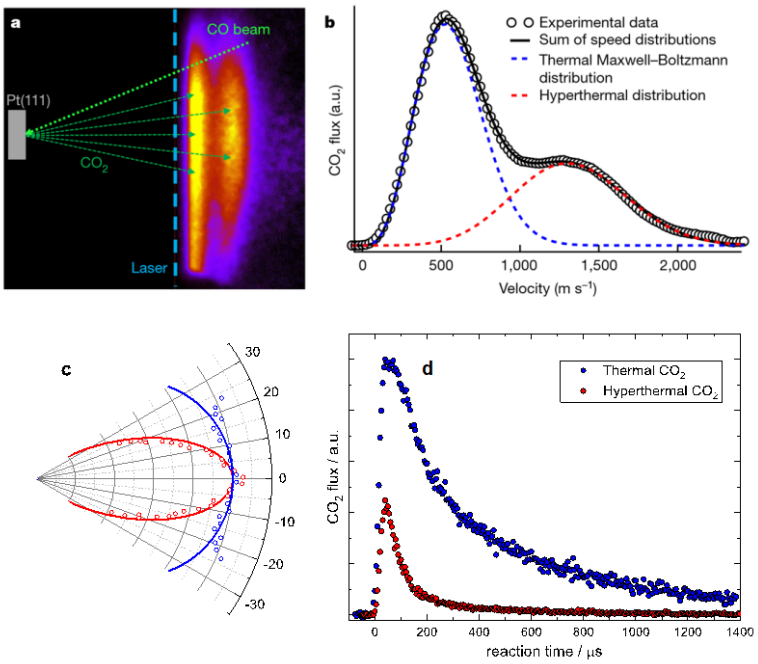

Figure 4: Ion imaging of chemical reaction products from CO oxidation on Pt(111) directly reveals the contribution of a thermal and a hyperthermal channel. *a) ion image of CO_2, obtained by scanning the focus of the ionization laser along the vertical blue dotted line, b) derived velocity distribution, c) derived angular distributions of the thermal (blue) and hyperthermal (red) components. d) The total CO_2 flux in each channel is obtained as a function of reaction time by scanning the time delay between the incident pulsed CO beam and the ionization laser, focused near the surface normal. The densities have been converted to flux using the measured velocities, the intensities have been corrected for differences in angular distributions, and the time axis has been corrected for product flight time. See Ref. 15 for further details of how such data is obtained. Figure reproduced with permission from Ref. 15, Nature Publishing Group.*

with reactant surface scattering is shown. The two beams pass between a repeller, initially held at ground, and another grounded grid. A laser pulse at the blue point ionizes reaction products desorbing from the surface; the laser beam is coplanar with the incident molecular beams. We refer to this hereafter as the probe laser. After a delay of 0–3 μs, the repeller is pulsed to a high voltage and the ions fly to the ion imaging detector. The ion image is then recorded for each pulse. The position where the ion is recorded reveals the velocity projected onto the plane defined by the molecular and laser beams. The in-plane probe laser geometry discriminates against products that scatter out of this plane. Further discrimination as well as mass resolution is obtained by pulsing the z-stack MCPs, thus employing mass-resolved slice imaging[21] and ensuring that the product molecule's absolute speed is obtained. This quantity is then multiplied by the signal intensity to obtain a flux intensity map. To improve velocity resolution, an Einzel lens placed after the grounded grid provides the capability to perform velocity map imaging[22].

Figure 4 presents typical results for CO oxidation on Pt(111). Panel a) shows an ion image obtained shortly after the adsorption of the CO pulse onto the partially oxidized Pt surface. The green arrows schematically indicate the velocity vectors of the desorbing CO_2 product, which is ionized by a pulsed laser at the position of the blue dashed line. The ion image clearly exhibits two contributions. The ions appearing furthest to the right are part of the hyperthermal channel;

those closer to the blue dashed line are the thermal channel. Such images can be analyzed as shown in panel b) to deconvolute the relative contributions of the thermal and hyperthermal channels. The ion images also yield the angular distributions of the two channels shown in panel c). The information contained in panels a–c corresponds to a snapshot of the reaction kinetics at a point in time of the kinetic trace defined by the delay between the CO pulse used to initiate the reaction and the probe laser pulse used to detect products. Similar information is collected throughout the entire range of delays necessary to observe the full kinetic trace shown in panel d. The kinetic trace for each channel has been integrated over the angular distribution and the measured densities have been converted to flux. The time axis has been corrected for the product flight time.

The experimentally derived quantities presented in Fig. 4d) are, to our knowledge, the first accurate measurements of the branching between different surface reaction pathways to products with different velocity and angular distributions. Using this approach, it was possible to obtain similar kinetic traces at a variety of oxygen coverages and surface temperatures. It was then possible to construct a simple kinetic model involving three reactions: one where both CO and O are bound at neighboring terrace sites—the so-called TT reaction, which gives rise to hyperthermal CO_2—and two reactions where O is bound at a step site and CO is bound either at a neighboring step or terrace site—the SS and the TS reactions, respectively, which give rise to thermal CO_2.

Figure 5a shows the three rate constants obtained both for Pt(111) and Pt(332) surfaces. The step density on the Pt(332) surface is approximately 66x higher than the measured step density on the Pt(111) surface. Although there is uncertainty concerning the step direction on the Pt(111) surface, differences in step direction do not appear to affect the observed reaction kinetics strongly: For both Pt(111) and (332), nearly identical rate constants are obtained for the

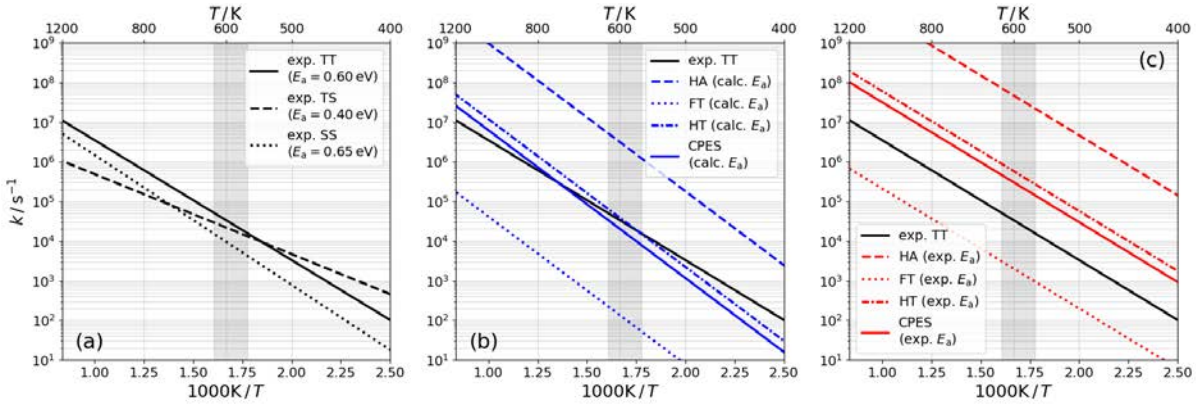

Figure 5: Measured and calculated rate constants for CO oxidation reactions occurring on steps or terraces. *. In each case, the rate constants, k, are defined in terms of the product formation rate as:* $rate = k\,\theta_{CO}\theta_O$. *TT & SS refer to the reaction with both O and CO on terrace, or step sites, respectively. TS is the reaction with O at a step and CO at a terrace. Panel (a) shows the measured rate constants for the three elementary oxidation reactions from Ref. 15. Results obtained from a Pt(111) surface with a 0.25% step density and those obtained from a Pt(332) crystal with 16.7% step density were nearly identical and the average is plotted here. In panels (b) and (c), the rate constant of the TT reaction (black solid line) is compared with a transition state theory calculation using a harmonic approximation (HA)[26], and with a free two-dimensional translator (FT) and a hindered translator (HT) approximation[29]. A complete potential energy sampling method calculation[29] is also shown. The theoretical rates in panel (b) are plotted with the calculated activation barrier and the rates in panel (c) have been adjusted to the experimentally determined activation barrier. The gray shaded region indicates the temperature range over which the experiments were performed.*

three reactions. These results provide rates of elementary reactions on a surface with multiple reaction sites. There are a few things we can learn from this.

First, we can investigate the importance of velocity resolved detection to obtaining accurate results on this problem. Figure 6 compares the results obtained should velocity information be unavailable (panel a), to that obtained with velocity-resolved kinetics experiments (panel b). Without velocity information (panel a), no density-to-flux conversion can be performed; hence,

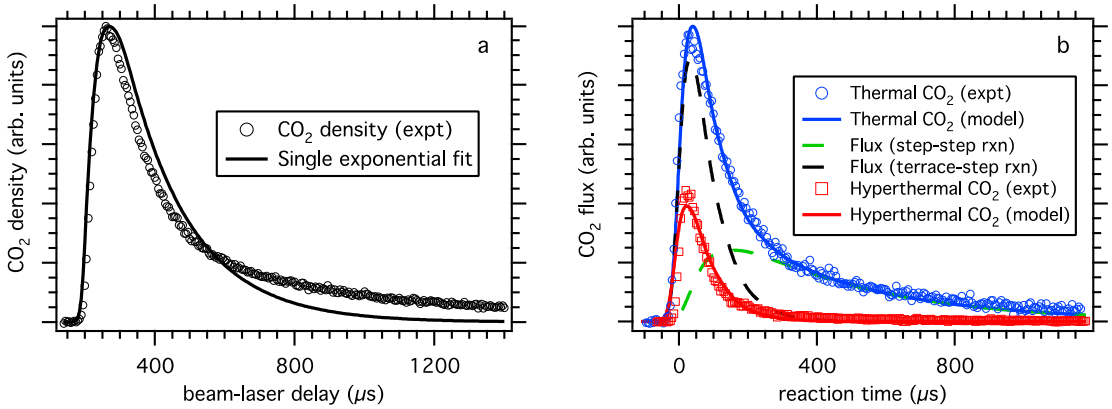

Figure 6: Comparison of the density vs. time trace (a) with the velocity-resolved CO_2 flux trace. *The data is from a Pt(111) surface at a temperature of 623 K and an oxygen coverage of 0.04 ML. The density trace (a) is obtained by integrating the total product density at angles within 5° of the surface normal. The CO_2 flux trace (b) is obtained from the velocity-resolved ion images as illustrated in Figure 4. The relative intensities of the two velocity-resolved channels has been corrected for differences in speed and angular distributions, and different kinetics for the two channels can be distinguished. This information enabled a quantitative fit to a model involving three elementary reactions: reactions on terraces (red curve), reactions of CO on terraces with O on steps (black dashed curve), and reactions of CO on steps with O on steps (green dashed curve). The data is obtained from Ref. 15.*

the *y*-axis represents the density of products near the surface normal as a function of delay between the molecular beam pulse of reactants and the ionization laser pulse. The information content of this data is clearly lower than that of panel b. It is not surprising that data like this obtained in previous work was fit assuming pseudo-first order rate equations—by default assuming a single reaction. In panel b, the velocity-resolved data reveals different kinetics for the thermal and hyperthermal channels, which led to the development of a site-resolved model for the elementary reaction steps. The hyperthermal channel, which arises from reactions on terraces, decays quickly whereas the thermal channel exhibits biexponential decay with a fast component (terrace-step reaction) that decays at the rate of the hyperthermal channel and a second component (step-step reaction) that decays at a slower rate. The temperature and oxygen coverage dependence of the reaction kinetics were obtained previously by temperature programmed reaction[23] and molecular beam reactive scattering[24]. In order to fit the data, it was necessary to allow the activation energy to vary with surface coverage. This required postulating that the energetic barrier to CO_2 formation varied by ~ 0.7 eV as the surface coverage of O atoms changed due to the influence of nearby adsorbed O atoms. We now know this is not correct.

In Ref. 15, it was shown that when velocity-integrated kinetic traces like those of Fig. 6a are fit with a pseudo first-order kinetic model (single exponential fit, Fig. 6a), the apparent reaction activation energy varies strongly with oxygen coverage over a similar range as that reported previously.[23,24] This comparison made an important point: if activation energies depend strongly on reactant concentration (in this case O-coverage), it is possible that this is a result of using the wrong chemical mechanism to fit the data. Figure 7 shows effective pseudo first-order activation energies obtained from the fit model (Table 1 of Ref. 15) as a function of surface temperature and oxygen coverage at low CO coverage. The effective activation energies in panel a are obtained from the overall decay rate of product signal, which reflects disappearance of CO via either reaction or desorption. The activation energy depends on O-coverage and surface temperature, varying over about 1 eV due to the dominance of different elementary processes at different temperatures and coverages. The effective activation energies for the oxidation reaction, obtained after correcting for the effects of desorption, are shown in panel b. The temperature and O-coverage range of various experiments and of industrially relevant catalysis are also indicated. (A direct comparison to the model may not be appropriate in all cases, since some experiments were performed at high CO coverage where poisoning of reactive sites may occur.)

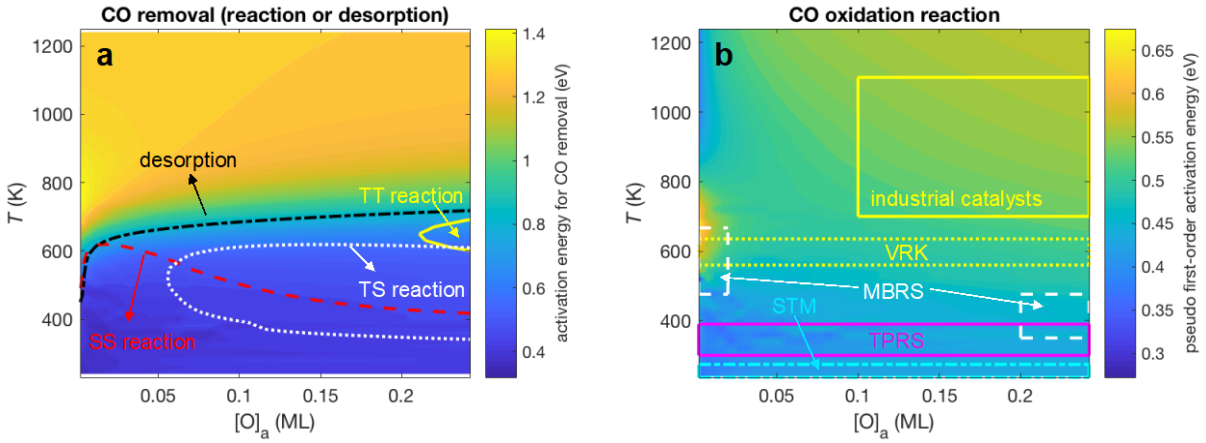

Figure 7: Temperature- and coverage-dependence of effective activation energies*. The pseudo first-order activation energy is obtained from the model in Table 1 of Ref. 15 (see text) and plotted for low CO coverage as a function of temperature and oxygen coverage. Shifts in the activation energy reflect shifts in the dominant rate-limiting process. The energies are calculated from* $-k_B\, dk_{eff}/dT^{-1}$*, where* $k_{eff} = P_f k_f + P_s k_s$ *is the weighted average of the "fast" rate (*k_f*, involving terrace CO), and the "slow" rate, (*k_s*, involving step-bound CO). (*P_f *and* P_s *are the fraction of* CO_2 *formed via the fast and slow decay channels, respectively.) The energies in panel a are obtained from the overall product decay so that they represent the activation energy for CO removal by reaction or desorption, whereas the energies in panel b include only the reactive processes. i.e. in panel a,* $k_f = k_0^T + k_1^{TS}\theta_S + k_2^{TT}\theta_{O,terr} + k_2^{TS}\theta_{O,step}$*, and* $k_s = k_0^S + k_2^{SS}\theta_{O,step}$*. (*$\theta_{O,terr}$*,* $\theta_{O,step}$*, and* θ_S *are the fractional coverage of oxygen on terraces, oxygen on steps, and unoccupied step sites, respectively; the elementary rate constants are defined as in Table 1 of Ref. 15). The isocurves in panel a represent the temperature and coverage at which the yield of each process amounts to 40% of the initial CO coverage. (Desorption is indicated by a black dash-dotted curve, the TT reaction by a yellow solid curve, the TS reaction by a white dotted curve and the SS reaction by a red dashed curve. See Fig 8.) In panel b, the rate constants defined similarly, but do not include desorption from terraces and steps (*k_0^T *and* k_0^S*, respectively). The boxes in panel b illustrate the temperature and coverage range relevant to industrial catalysis (yellow solid box), and at which kinetic measurements have been performed via Scanning Tunneling Microscopy (STM, dash-dotted cyan box)[44], Temperature Programmed Reaction Spectrometry (TPRS, solid magenta box)[23], Modulated Beam Relaxation Spectrometry (MBRS, white dashed boxes)[24], and Velocity Resolved Kinetics (VRK, yellow dotted box)[15].*

Figure 7 illustrates how easily kinetic measurement can be misinterpreted—the absence of velocity resolved data easily leads to an assumption of an incorrect kinetic mechanism, where the activation energy depends on the reactant concentration and surface temperature. Moreover, the activation energy derived will depend on the temperatures and O-coverages where the experiment could be carried out.

In stark contrast to this, the kinetic model that has been derived from velocity resolved kinetics explains the roles of different reaction sites and provides activation energies that are independent of O-coverage and surface temperature. Figure 8 shows this for CO oxidation on Pt(111) with 0.25% step density. The four panels show the fraction of adsorbed CO that undergoes desorption (panel a) or oxidation via the three elementary reactions included in the model (panels b–d). Nearly all kinetics work has been carried out in the temperature range from 230–670 K. We note that step reactions dominate, despite the fact that the Pt(111) surface used in this work had a measured surface step density of far less than 1% of a monolayer. Clearly, the vast majority of reactivity proceeds via CO adsorption at terraces followed by diffusion to steps, where CO_2 is formed.

Typical commercial applications of Pt catalyzed CO oxidation occur in the region between 700 K and 1100 K. (Note, however, that the micro-kinetic model used in Fig. 8 is for a Pt(111) surface under UHV conditions and cannot make quantitative predictions for industrial catalysts.) Here, reactions at terraces are much more important and the CO oxidation probability is reduced. This is easy to understand. At high temperatures CO desorption is much faster than diffusion and we enter a regime where diffusion plays no role. Reaction occurs at the point of adsorption and desorption reduces the overall reaction probability. Since the low-oxygen-coverage MBRS measurements of ref. 24 monitored only the CO_2 normal to the surface, they could easily have been biased in favor of the TT reaction, whose contribution increases at high temperatures. This could easily have led to an artificially high apparent activation energy for the Langmuir-Hinshelwood step (1.05 eV, versus 0.67 eV at the most in Fig. 7b), again showing the importance of a correct mechanistic model.

This simple mechanistic insight also suggests that catalyst studies using scanning tunneling microscopy, which are typically performed at temperatures below 300 K, must be interpreted very carefully when conclusions from that work might be applied at higher reaction temperatures. See the discussion of oxygen island formation and its effect on reactivity presented below.

The analysis makes a fundamental point: surface kinetics may be simpler than we believed. If we employ an approximation of homogeneous reactant mixing and if we further assume that activation energies are independent of reactant concentration, we would expect an expression for the rate of a single elementary CO oxidation reaction would take the following form:

$$\text{rate} = Ae^{-E_A/RT}\theta_{CO}\theta_O.$$

The simplicity of such a form is attractive. But if real physical effects exist where the barriers to chemical reactions depend on surface concentrations, then the problem is more complex.

Although a mild dependence on surface coverage cannot be ruled out due to experimental uncertainty, the results of this study suggest that for the CO oxidation reaction such effects are minor. This may seem surprising as adsorption energies certainly do depend on surface coverage, an effect that has been explained by repulsive forces between densely packed adsorbates in a monolayer – see for example Ref. 25. However, if there is a repulsive interaction that lowers the adsorption energy of reactants, there will often also be repulsive interactions that lower the adsorption energy of the transition state and of the surface-bound product to some extent. This

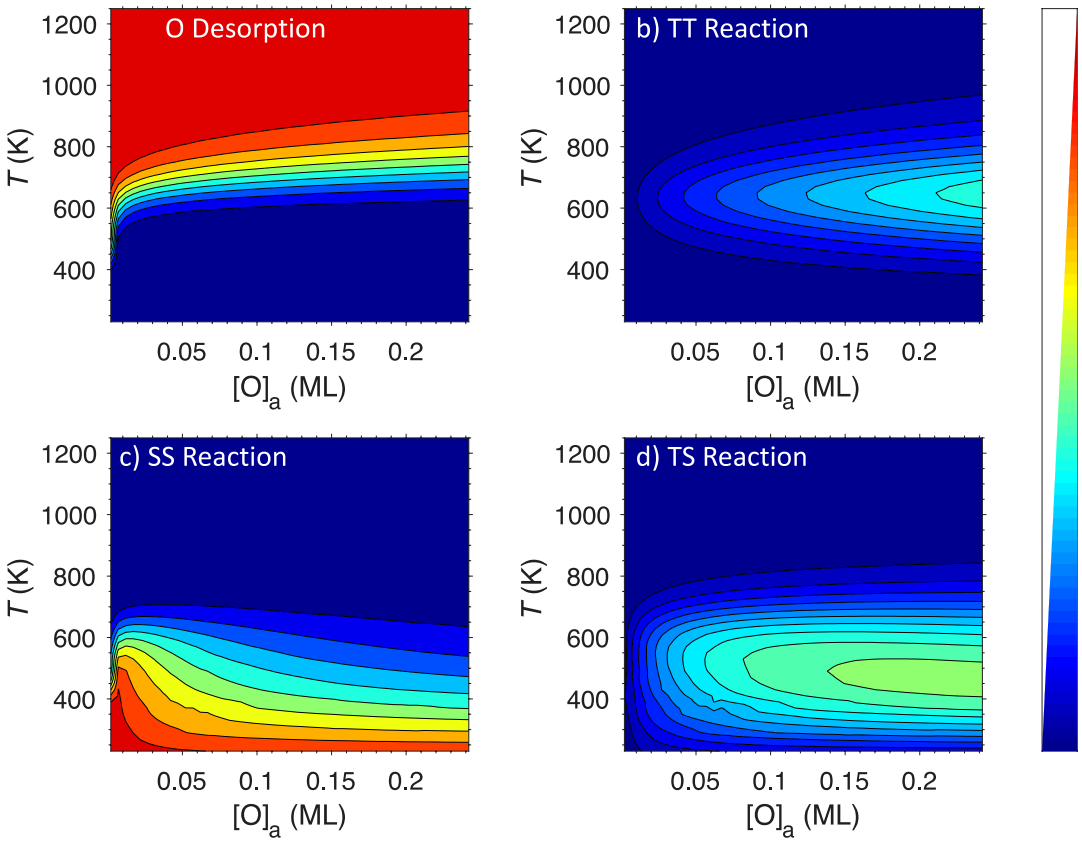

Figure 8: The role of steps in a surface reaction. *The micro-kinetic model for CO oxidation on Pt(111) reveals that a large fraction of the products are formed at step defects, even when the step density is low, and how the role of steps changes with temperature and O coverage. The four panels show the fraction of CO that undergoes desorption (a) or that is oxidized via the three different elementary reactions (TT, SS, and TS) included in the model of Ref. 15 (panels b–d). The fractions are calculated from the parameters given in Table 1 of Ref. 15 in the low CO coverage limit.*

may mean that activation energies that are coverage independent, or nearly so, are more common than presently believed. While exceptions will undoubtedly be found, we should in future be cautious about interpreting data using models where the activation energy changes strongly with coverage. The kinetics studies presented here on three CO oxidation reactions show no strong coverage dependence, which suggests that previously reported coverage dependence may have been an artefact due to the assumption of an overly simple mechanism.

Perhaps the most significant idea we would like to convey to the reader is that we are now close to being able to develop accurate theories of surface reaction rates based on experimental benchmarks. Figures 5b and c compare the experimentally derived rate constant for the TT reaction (most commonly assumed in theoretical treatments of CO oxidation on metals) to that obtained theoretically. The dashed blue line in panel b shows calculations from Eichler[26] using methods that would be commonly used today. Here, density functional theory is used to calculate the energy and structure of the transition state of the TT reaction. Once the transition state structure

is found, its vibrational frequencies are calculated. This provides the necessary input for transition state theory, the most commonly used and successful model of gas-phase reaction rates.

The deviation with experiment is between one and two orders of magnitude, better at low temperature than at high temperature. The theory does not give the proper temperature dependence. This is not the most fundamental problem as the RPBE functional used in this calculation has been found to overestimate the height of reaction barriers in other systems[27]. One assumes that, sooner or later, better functionals will be found that provide more accurate barrier heights. If we simply adjust the barrier height to match the experimental activation energy (red dashed line, panel c), the agreement with experiment is significantly worsened.

This line of reasoning clearly shows that the analysis of Eichler introduced large errors in the Arrhenius pre-exponential factor, a quantity that reflects the entropy difference between reactants and the transition state. It would appear that Eichler pursued a model where the reactants have far too little entropy. A closer look at the assumptions of that paper reveals that the influence of CO diffusive entropy was not considered. At the temperatures relevant to this reaction, the CO molecule explores a wide range of configuration space before finding the transition state as it wanders about the surface looking for its pathway to products[28]. The use of a free translator model (dotted lines in Fig 5b and c) significantly decreases the rate constant to bring it 1–2 orders of magnitude below experiment. A hindered translator model (dash-dotted lines) exhibits better agreement with experiment. Jørgensen *et al*. recently introduced a first principles approach to dealing with this sort of problem: the complete potential energy sampling method (CPES)[29]. We applied this method to obtain the rate constants shown as solid blue and red lines in Fig. 5b and c. The resulting rate constant is in good agreement with experiment when the RPBE energies are assumed (panel b), but this is likely due to cancellation of error. When the CPES prefactor is used with experimentally determined activation energies, the resulting rate constants overestimate the experiment by an order of magnitude (panel c).

The remaining order of magnitude difference between experiment and theory poses questions that must be addressed in future research. Improved electronic structure calculations are clearly needed that provide the properties of the transitions state more accurately. Beyond this, the fundamental assumptions of transition state theory need to be tested. Transition state theory assumes that once the transition state is crossed it can never be re-crossed; hence, it always provides a rate that is higher than or equal to the actual rate. The importance of transition state re-crossing in CO oxidation—or any other surface reaction—is still unknown. Another fundamental assumption of the transition state theory is its assumption of the absence of frictional

forces in the transition state traversal. Such forces can arise from interactions between the O and C atoms with the electrons of the platinum, where the Born-Oppenheimer approximation fails[11-13] and electron-hole pair excitation robs energy from the nuclear motion[30] through the transition state, reducing reaction probability.

Other methods of interest

The focus of this short perspective has been the velocity resolved approach to studying kinetics of elementary reactions on well-defined model catalytic surfaces. However, velocity resolved methods are not always necessary to gain insights into heterogeneous catalysis. Understanding catalysis also requires information on adsorbate stabilities. Due to its simplicity, there is a vast literature of Temperature Programmed Desorption (TPD)-based adsorbate binding energies; but, we caution these may be subject to large errors, especially when assumptions about desorption prefactors are made. Ways to extract the most accurate information possible from TPD have been discussed[31-34]. The most accurate binding energies can be derived when TPD experiments are conducted over a wide range of heating rates, when better prefactor estimates are available or by numerical fitting of the entire TPD curve.

Equilibrium measurements of coverage vs. temperature and pressure are widely used to obtain reliable adsorption energies[31,32]. When equilibrium cannot be realized, single crystal adsorption calorimetry (SCAC) can be used to measure the heat input induced by adsorption directly[35-37]. A molecular beam is used to deliver a series of weak pulses ($\approx$ 0.01 ML) of the molecule of interest to a single crystal sample and the temperature rise of the sample is measured. The most sensitive method to date uses a pyroelectric detector in contact with the back of the single crystal sample to measure the temperature rise[36]. The adsorption probability for the beam pulse is determined by measuring the fraction of the beam that reflects, and the heat adsorbed is calibrated by adsorption of light from a laser beam, directed down the same path as the molecular beam. Thus, the heat released by the adsorption of a known number of molecules at a certain coverage can be determined for both molecular adsorption and dissociative adsorption.

There are also a variety of alternatives for measuring kinetics. For example, in Temperature Programmed Reaction Spectrometry (TPRS)[38], the system is first prepared with a given concentration of reactants at low temperature. Desorbed reaction products are observed while providing a linear ramp of the surface temperature. This method has been successful for catalyst

characterization, understanding reaction mechanisms, determining kinetic data, rapid evaluation of catalyst activity, and measuring surface areas of adsorption[39].

Alternatively, one may use surface sensitive detection methods to follow the concentration of adsorbed reactants, intermediates and products as a function of reaction time. This approach also provides the kinetic trace; unfortunately, available techniques like Infrared Reflection Absorption Spectroscopy (IRAS)[40,41], X-Ray Photoelectron Spectroscopy (XPS)[42,43] and Scanning Tunneling Microscopy (STM)[44] tend to be restricted to conditions where reaction rates are slow working at low surface temperatures that are often far from those of practical interest and exhibit qualitatively different kinetic mechanisms.

Here again, the comparison of methods when applied to CO oxidation on Pt surfaces is interesting. When rates of CO oxidation are measured with sub-millisecond time resolution at T_s = 500–700 K, (see Fig. 6) kinetic models based on complete reactant mixing are successful. Kinetic analysis starts with the mathematical Ansatz $\Phi_{CO_2} = k \cdot \theta_O \cdot \theta_{CO}$. Studies with STM and XPS were used to observe the reaction at $T_s \approx$ 250 K. By pre-adsorbing O and exposing to CO in the background gas, time resolved STM images showed the reaction rate was proportional to the perimeter length of O-islands[44]. Synchrotron based XPS was also used to follow the reaction under similar conditions and gave consistent results[43]. At low T_s, the rate took the form $k \cdot \theta_O^{0.55}$. These results highlight real differences in the way reactions occur at low temperatures and the danger of extrapolating results to high temperature conditions closer to real catalytic conditions.

Another kinetics approach is Modulated Beam Relaxation Spectrometry (MBRS)[45], which can follow much faster reactions. Here, reactants are delivered to the surface as periodic pulses; the delay of the product signal is measured as a phase lag relative to these pulses. The phase lag between the product and reactant signal is related to the rate of reaction. Analysis requires formulating a kinetic model of the reaction and adjusting the parameters of the model to achieve agreement with the observed product signals. If the kinetic model is not correct, it may still be possible to get agreement with the observed product signal over the range of conditions probed, but the inferred kinetic parameters will be incorrect and not useful for calculating rates under other conditions. Nevertheless, when properly applied the MBRS method can be a powerful tool.

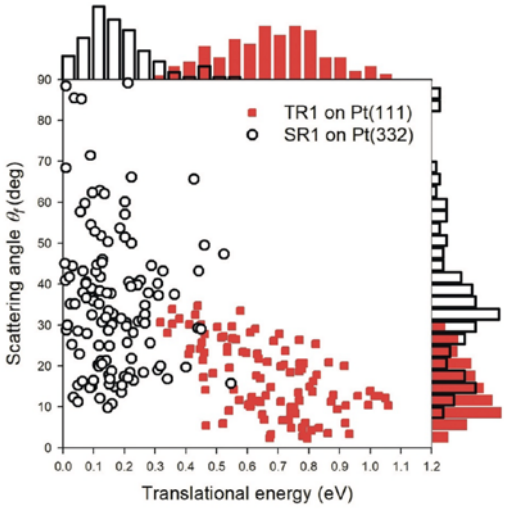

Figure 9: Results of ab initio molecular dynamics trajectory calculations used to obtain the final angular and translational energy distributions from the site-specific post-transition state dynamics of CO oxidation on Pt. *TR1 (red filled squares) represents results from the preferred path on the Pt(111) terrace and SR1 (open circles) represents the preferred reaction path at a Pt(332) step site. The calculated angular and speed distributions are in semi-quantitative agreement with experiment. Figure reprinted with permission from Fig. 3 of Ref. 16.*

Outlook

The improvements in computational chemistry we have a witnessed over the last three decades are nothing short of revolutionary. State-of-the-art problems for theory in the 1980s included the $H + H_2 \rightarrow H_2 + H$ reaction. Today, we can simulate the adsorption of H-atoms to a solid metal surface[30] or to graphene[46], describing the dynamics that occur on the femtosecond timescale with atomic-scale precision. The development of new catalysts has traditionally been achieved by experimental empiricism. In future, this will be led and guided by theoretical simulations with predictive power[47]. The recent velocity-resolved kinetics results on CO oxidation have already led to new synergy between theory and experiment that help explain the site-specific reaction dynamics. A DFT-based *ab initio* molecular dynamics simulation found that CO_2 formed on the Pt(111) terrace desorbs directly, whereas CO_2 formed on a Pt(332) step site is temporarily trapped in a shallow chemisorption well for enough time for the translational energy to thermalize with the surface, giving rise to the thermal and hyperthermal reaction channels observed experimentally (see Fig. 9).[16]

Modern synchrotron XPS- and STM-based methods capable of operating at high or near-ambient pressure have revealed significant structural changes to the surface that make it challenging to connect UHV experiments on model catalysts to "real-world" problems.[48] Two examples that address this so-called "pressure gap" are worth special note. The first employed experimental results obtained in ultrahigh vacuum experiments on single crystal metals together with DFT based theory[49-54], to devise a kinetic model for a high pressure reactor comprised on nanoparticles. The extrapolation from UHV and single crystals to high pressure and nanoparticles has been referred to as the pressure and material gaps, but – in the words of these authors – "…they actually comprise a knowledge continuum, which can be understood from basic principles". In that study, basic knowledge derived from the study of model systems could be used to predict product selectivity for oxygen-assisted esterification of methanol over gold nanopar-

ticle catalysts under high pressure catalytic conditions[55]. This successful micro-kinetic modeling of catalytic reactions across a wide set of reaction conditions provides a framework for future studies of rational catalysis design.

In related work, micro-kinetic modeling with Monte-Carlo kinetics methods based on rate constants derived from first principles electronic structure theory was used to describe catalytic CO oxidation on RuO_2[56]. Results could be compared to experiments carried out at high temperatures and pressures and the theory was in good agreement with observations. Laser Induced Fluorescence (LIF) imaging of CO oxidation under elevated pressure conditions on a curved Pd crystal also revealed micro-kinetic information about the influence of different step types, which could be understood by comparison of experiment with theory.[57] Such work shows the way forward despite the fact that fundamental questions remain due to the difficulties in testing these theoretical approaches against accurately measured reaction rates – a theme of this paper. But these tests will be made and where theories are found to be lacking new ideas will emerge. Nothing is needed to ensure this bright future other than support of the chemical community still struggling with the daunting problem of unraveling the secrets of heterogeneous catalysis.

In the introduction to this paper, we documented the costs of inadequate heterogeneous catalysis to just a single company to be on the order of several 100 billion $US. Had the leaders of those same companies had greater vision, they might have invested a small fraction of these losses in the basic research of heterogeneous catalysis to improve our ability to design new catalysts by principles based on physical understanding. That investment together with one for in-house proprietary applications research, surely would have led to technological improvements that would have offered more attractive solutions than defeat devices. To put it another way, had the EU in cooperation with European automakers invested just 1% of VWs eventual losses—one billion € per year—in research on catalytic processes, it would have been among the largest research initiative in the world. Such research would surely have had an impact, not only on the value of VWs stock, but on tens of thousands of people whose lives ended prematurely due to automobile air pollution.

References

1 Anenberg, S. C. *et al.* Impacts and mitigation of excess diesel-related NO_x emissions in 11 major vehicle markets. *Nature* **545**, 467-471, doi:10.1038/nature22086 (2017).

2 Thompson, G. J. *In-Use Emissions Testing of Light-Duty Diesel Vehicles in the United States* <https://www.theicct.org/sites/default/files/publications/WVU_LDDV_in-use_ICCT_Report_Final_may2014.pdf> (2014).

513 3 Fortune. *VW Fights Investors as Diesel-Scandal Cost Could Top $35 Billion*,
514 <http://fortune.com/2018/09/08/volkswagen-vw-diesel-scandal/> (2018).

515 4 Ling, S., Kho, F., Lim, J. & Chu, C. *Driving Volkswagen AG into the future*,
516 <https://foster.uw.edu/wp-content/uploads/2014/12/PP-B3-Singapore-NUS.pdf> (2016).

517 5 Nørskov, J. K., Bligaard, T., Rossmeisl, J. & Christensen, C. H. Towards the computational
518 design of solid catalysts. *Nature Chemistry* **1**, 37-46, doi:10.1038/nchem.121 (2009).

519 6 Crutzen, P. J. My life with O_3, NO_x, and other YZO_x compounds (Nobel lecture). *Angewandte*
520 *Chemie-International Edition* **35**, 1758-1777, doi:10.1002/anie.199617581 (1996).

521 7 Weber, M. *et al.* Total ozone trends from 1979 to 2016 derived from five merged observational
522 datasets - the emergence into ozone recovery. *Atmos. Chem. Phys.* **18**, 2097-2117,
523 doi:10.5194/acp-18-2097-2018 (2018).

524 8 Roy, S., Hegde, M. S. & Madras, G. Catalysis for NO_x abatement. *Appl. Energy* **86**, 2283-2297,
525 doi:10.1016/j.apenergy.2009.03.022 (2009).

526 9 Kurylo, M. J. & Orkin, V. L. Determination of atmospheric lifetimes via the measurement of
527 OH radical kinetics. *Chem. Rev.* **103**, 5049-5076, doi:10.1021/cr020524c (2003).

528 10 Vereecken, L. & Francisco, J. S. Theoretical studies of atmospheric reaction mechanisms in the
529 troposphere. *Chem. Soc. Rev.* **41**, 6259-6293, doi:10.1039/c2cs35070j (2012).

530 11 Wodtke, A. M. Electronically non-adiabatic influences in surface chemistry and dynamics.
531 *Chem. Soc. Rev.* **45**, 3641-3657, doi:10.1039/c6cs00078a (2016).

532 12 Golibrzuch, K., Bartels, N., Auerbach, D. J. & Wodtke, A. M. in *Annual Review of Physical*
533 *Chemistry, Vol 66* Vol. 66 *Annual Review of Physical Chemistry* (eds M. A. Johnson & T. J.
534 Martinez) 399-425 (Annual Reviews, 2015).

535 13 Silva, M., Jongma, R., Field, R. W. & Wodtke, A. M. The dynamics of "stretched molecules":
536 Experimental studies of highly vibrationally excited molecules with stimulated emission
537 pumping. *Annu. Rev. Phys. Chem.* **52**, 811-852, doi:10.1146/annurev.physchem.52.1.811
538 (2001).

539 14 Becker, C. A., Cowin, J. P., Wharton, L. & Auerbach, D. J. CO_2 product velocity distributions
540 for CO oxidation on platinum. *The Journal of Chemical Physics* **67**, 3394,
541 doi:10.1063/1.435289 (1977).

542 15 Neugebohren, J. *et al.* Velocity-resolved kinetics of site-specific carbon monoxide oxidation on
543 platinum surfaces. *Nature* **558**, 280--283, doi:10.1038/s41586-018-0188-x (2018).

544 16 Zhou, L., Kandratsenka, A., Campbell, C. T., Wodtke, A. M. & Guo, H. Origin of thermal and
545 hyperthermal CO_2 from CO oxidation on Pt surfaces: The role of post-transition-state dynamics,
546 active sites, and chemisorbed CO_2. *Angew. Chem. Int. Ed.* **58**, 6916-6920,
547 doi:10.1002/anie.201900565 (2019).

548 17 Segner, J., Campbell, C. T., Doyen, G. & Ertl, G. Catalytic oxidation of CO on Pt(111): The
549 influence of surface defects and composition on the reaction dynamics. *Surf. Sci.* **138**, 505-523,
550 doi:10.1016/0039-6028(84)90262-0 (1984).

551 18 There is a great deal buried in this simple sentence. The 1977 work of Ref. 14 used a single
552 chopper wheel. Here, one chopper wouldn't do. To measure velocity resolved kinetics would
553 require a way to initiate the reaction at a known time (e.g. chopped supersonic beam or pulsed

supersonic beam) and a way to measure the velocity of products. Measuring product velocity could be done with a chopper or velocity selector in the path of the products, i.e. after the surface. The chopper after the surface would have to be synchronized with the initiating pulse to get the velocity resolved kinetic trace. A pulse picker or equivalent electronics would be needed to chop the product distribution at a certain reaction time. Corrections for flight time from the input chopper to the surface and from the surface to the exit chopper would be quite difficult. A rotatable detector is also needed to obtain the angular distribution information. Each double chopper implemented velocity resolved kinetics measurement would have to be repeated at a number of desorption angles. In light of this, it is perhaps easier to see how truly wonderful it is to have a detector like slice ion-imaging that intrinsically gives the product momentum - both speed and direction - with every laser shot.

19 Chandler, D. W. & Houston, P. L. TWO-DIMENSIONAL IMAGING OF STATE-SELECTED PHOTODISSOCIATION PRODUCTS DETECTED BY MULTIPHOTON IONIZATION. *Journal of Chemical Physics* **87**, 1445-1447, doi:10.1063/1.453276 (1987).

20 Heck, A. J. R. & Chandler, D. W. IMAGING TECHNIQUES FOR THE STUDY OF CHEMICAL-REACTION DYNAMICS. *Annual Review of Physical Chemistry* **46**, 335-372, doi:10.1146/annurev.pc.46.100195.002003 (1995).

21 Gebhardt, C. R., Rakitzis, T. P., Samartzis, P. C., Ladopoulos, V. & Kitsopoulos, T. N. Slice imaging: A new approach to ion imaging and velocity mapping. *Review of Scientific Instruments* **72**, 3848-3853, doi:Doi 10.1063/1.1403010 (2001).

22 Eppink, A. & Parker, D. H. Velocity map imaging of ions and electrons using electrostatic lenses: Application in photoelectron and photofragment ion imaging of molecular oxygen. *Rev. Sci. Instrum.* **68**, 3477-3484, doi:10.1063/1.1148310 (1997).

23 Gland, J. L. & Kollin, E. B. Carbon monoxide oxidation on the Pt(111) surface: Temperature programmed reaction of coadsorbed atomic oxygen and carbon monoxide. *The Journal of Chemical Physics* **78**, 963, doi:10.1063/1.444801 (1983).

24 Campbell, C. T., Ertl, G., Kuipers, H. & Segner, J. A molecular-beam study of the catalytic-oxidation of CO on a Pt(111) surface. *J. Chem. Phys.* **73**, 5862-5873, doi:10.1063/1.440029 (1980).

25 Yeo, Y. Y., Vattuone, L. & King, D. A. Calorimetric heats for CO and oxygen adsorption and for the catalytic CO oxidation reaction on Pt{111}. *J. Chem. Phys.* **106**, 392-401, doi:10.1063/1.473203 (1997).

26 Eichler, A. CO oxidation on transition metal surfaces: reaction rates from first principles. *Surface Science* **498**, 314-320, doi:10.1016/s0039-6028(01)01805-2 (2002).

27 Diaz, C. *et al.* Chemically accurate simulation of a prototypical surface reaction: H_2 dissociation on Cu(111). *Science* **326**, 832-834, doi:10.1126/science.1178722 (2009).

28 Sprowl, L. H., Campbell, C. T. & Arnadottir, L. Hindered translator and hindered rotor models for adsorbates: Partition functions and entropies. *Journal of Physical Chemistry C* **120**, 9719-9731, doi:10.1021/acs.jpcc.5b11616 (2016).

29 Jørgensen, M. & Gronbeck, H. Adsorbate entropies with complete potential energy sampling in microkinetic modeling. *Journal of Physical Chemistry C* **121**, 7199-7207, doi:10.1021/acs.jpcc.6b11487 (2017).

30 Bünermann, O. *et al.* Electron-hole pair excitation determines the mechanism of hydrogen atom adsorption. *Science* **350**, 1346-1349, doi:10.1126/science.aad4972 (2015).

31 Campbell, C. T. & Sellers, J. R. V. Enthalpies and entropies of adsorption on well-defined oxide surfaces: Experimental measurements. *Chem. Rev.* **113**, 4106-4135, doi:10.1021/cr300329s (2013).

32 Silbaugh, T. L. & Campbell, C. T. Energies of Formation Reactions Measured for Adsorbates on Late Transition Metal Surfaces. *Journal of Physical Chemistry C* **120**, 25161-25172, doi:10.1021/acs.jpcc.6b06154 (2016).

33 Habenschaden, E. & Kuppers, J. Evaluation of flash desorption spectra. *Surf. Sci.* **138**, L147-L150, doi:10.1016/0039-6028(84)90488-6 (1984).

34 King, D. A. Thermal desorption from metal surfaces. *Surf. Sci.* **47**, 384-402, doi:10.1016/0039-6028(75)90302-7 (1975).

35 Borroni-Bird, C. E., Al-Sarraf, N., Andersson, S. & King, D. A. Single crystal adsorption microcalorimetry. *Chem. Phys. Lett.* **183**, 516-520, doi:10.1016/0009-2614(91)80168-w (1991).

36 Stuckless, J. T., Frei, N. A. & Campbell, C. T. A novel single-crystal adsorption calorimeter and additions for determining metal adsorption and adhesion energies. *Rev. Sci. Instrum.* **69**, 2427-2438, doi:10.1063/1.1148971 (1998).

37 Campbell, C. T. Energies of adsorbed catalytic intermediates on transition metal surfaces: Calorimetric measurements and benchmarks for theory. *Acc. Chem. Res.* **52**, 984-993, doi:10.1021/acs.accounts.8b00579 (2019).

38 Madix, R. J. & Telford, S. G. The kinetic isotope effect for C-H bond activation on Cu(110): The effects of tunnelling. *Surf. Sci.* **277**, 246-252, doi:10.1016/0039-6028(92)90765-x (1992).

39 Falconer, J. L. & Schwarz, J. A. Temperature-programmed desorption and reaction: Applications to supported catalysts. *Catal. Rev.-Sci. Eng.* **25**, 141-227, doi:10.1080/01614948308079666 (1983).

40 Xu, J. Z. & Yates, J. T. Catalytic oxidation of CO on Pt(335): A study of the active site. *J. Chem. Phys.* **99**, 725-732, doi:10.1063/1.465745 (1993).

41 Zaera, F. New advances in the use of infrared absorption spectroscopy for the characterization of heterogeneous catalytic reactions. *Chem. Soc. Rev.* **43**, 7624-7663, doi:10.1039/c3cs60374a (2014).

42 Fuhrmann, T. *et al.* Activated adsorption of methane on Pt(111) - an *in situ* XPS study. *New J. Phys.* **7**, 19, doi:10.1088/1367-2630/7/1/107 (2005).

43 Papp, C. & Steinruck, H. P. In situ high-resolution X-ray photoelectron spectroscopy - Fundamental insights in surface reactions. *Surf. Sci. Rep.* **68**, 446-487, doi:10.1016/j.surfrep.2013.10.003 (2013).

44 Wintterlin, J., Völkening, S., Janssens, T. V. W., Zambelli, T. & Ertl, G. Atomic and macroscopic reaction rates of a surface-catalyzed reaction. *Science* **278**, 1931--1934, doi:10.1126/science.278.5345.1931 (1997).

45 Schwarz, J. A. & Madix, R. J. Modulated beam relaxation spectrometry: Its application to the study of heterogeneous kinetics. *Surf. Sci.* **46**, 317-341, doi:10.1016/0039-6028(74)90260-x (1974).

46 Jiang, H. Y. *et al.* Imaging covalent bond formation by H-atom scattering from graphene. *Science* **364**, 379-382 (2019).

47 Reuter, K. & Metiu, H. in *Handbook of Materials Modeling.* (ed Yip S. Andreoni W.) (Springer, Cham, 2018).

48 van Spronsen, M. A., Frenken, J. W. M. & Groot, I. M. N. Surface science under reaction conditions: CO oxidation on Pt and Pd model catalysts. *Chem. Soc. Rev.* **46**, 4347-4374, doi:10.1039/C7CS00045F (2017).

49 Xu, B. J., Madix, R. J. & Friend, C. M. Predicting gold-mediated catalytic oxidative-coupling reactions from single crystal studies. *Acc. Chem. Res.* **47**, 761-772, doi:10.1021/ar4002476 (2014).

50 Stowers, K. J., Madix, R. J. & Friend, C. M. From model studies on Au(111) to working conditions with unsupported nanoporous gold catalysts: Oxygen-assisted coupling reactions. *J. Catal.* **308**, 131-141, doi:10.1016/j.jcat.2013.05.033 (2013).

51 Xu, B. J., Haubrich, J., Baker, T. A., Kaxiras, E. & Friend, C. M. Theoretical study of O-assisted selective coupling of methanol on Au(111). *Journal of Physical Chemistry C* **115**, 3703-3708, doi:10.1021/jp110835w (2011).

52 Xu, B. J. & Friend, C. M. Oxidative coupling of alcohols on gold: Insights from experiments and theory. *Faraday Discuss.* **152**, 307-320, doi:10.1039/c1fd00015b (2011).

53 Outka, D. A. & Madix, R. J. Acid-base and nucleophilic chemistry of atomic oxygen on the Au(110) surface: Reactions with formic acid and formaldehyde. *Surf. Sci.* **179**, 361-376, doi:10.1016/0039-6028(87)90063-x (1987).

54 Wachs, I. E. & Madix, R. J. The surface intermediate H_2COO. *Appl. Surf. Sci.* **5**, 426-428, doi:10.1016/0378-5963(80)90106-3 (1980).

55 Reece, C., Redekop, E. A., Karakalos, S., Friend, C. M. & Madix, R. J. Crossing the great divide between single-crystal reactivity and actual catalyst selectivity with pressure transients. *Nature Catalysis* **1**, 852-859, doi:10.1038/s41929-018-0167-5 (2018).

56 Reuter, K. & Scheffler, M. First-principles kinetic Monte Carlo simulations for heterogeneous catalysis: Application to the CO oxidation at RuO_2(110). *Physical Review B* **73**, 045433, doi:10.1103/PhysRevB.73.045433 (2006).

57 Blomberg, S. *et al.* Strain dependent light-off temperature in catalysis revealed by planar Laser-Induced Fluorescence. *ACS Catalysis* **7**, 110-114, doi:10.1021/acscatal.6b02440 (2017).

1. Highlighted references

Nørskov, J. K., Bligaard, T., Rossmeisl, J. & Christensen, C. H. Towards the computational design of solid catalysts. *Nature Chemistry* **1**, 37-46, doi:10.1038/nchem.121 (2009).

Neugebohren, J. et al. Velocity-resolved kinetics of site-specific carbon monoxide oxidation on platinum surfaces. *Nature* **558**, 280--283, doi:10.1038/s41586-018-0188-x (2018).

Jørgensen, M. & Gronbeck, H. Adsorbate Entropies with Complete Potential Energy Sampling in Microkinetic Modeling. *Journal of Physical Chemistry C* **121**, 7199-7207, doi:10.1021/acs.jpcc.6b11487 (2017).

Wintterlin, J., Völkening, S., Janssens, T. V. W., Zambelli, T. & Ertl, G. Atomic and Macroscopic Reaction Rates of a Surface-Catalyzed Reaction. *Science* **278**, 1931--1934, doi:10.1126/science.278.5345.1931 (1997).

Reece, C., Redekop, E. A., Karakalos, S., Friend, C. M. & Madix, R. J. Crossing the great divide between single-crystal reactivity and actual catalyst selectivity with pressure transients. *Nature Catalysis* **1**, 852-859, doi:10.1038/s41929-018-0167-5 (2018).

Reuter, K. & Scheffler, M. First-principles kinetic Monte Carlo simulations for heterogeneous catalysis: Application to the CO oxidation at RuO2(110). *Physical Review B* **73**, 045433, doi:10.1103/PhysRevB.73.045433 (2006).

Xu, B. J., Madix, R. J. & Friend, C. M. Predicting Gold-Mediated Catalytic Oxidative-Coupling Reactions from Single Crystal Studies. *Acc. Chem. Res.* **47**, 761-772, doi:10.1021/ar4002476 (2014).

Glossary

Langmuir-Hinshelwood mechanism: A common reaction mechanism in heterogeneous catalysis comprising four steps: adsorption of reactants to the catalyst including possibly dissociation of reactant(s) followed by diffusion bringing reactants together and reaction followed by product desorption.

Acknowledgements

AMW gratefully acknowledges support from the Alexander von Humboldt Foundation. We acknowledge support from the Deutsche Forschungsgemeinschaft (DFG) and the Ministerium für Wissenschaft und Kultur (MWK) Niedersachsen, and the Volkswagenstiftung under Grant No. INST 186/952-1, CTC acknowledges support for this work by the US National Science Foundation under Grant No. CHE-1665077. TNK acknowledges the European Research Council (ERC) under the European Union's Horizon 2020 research and innovation programme (grant agreement No. [833404]). DB thanks the BENCh graduate school, funded by the Deutsche Forschungsgesellschaft (DFG, German Research Foundation) – 389479699/GRK2455.

704

705